JOURNAL OF VIROLOGY, Feb. 2007, p. 2078–2082 Vol. 81, No. 4
0022-538X/07/$08.00+0 doi:10.1128/JVI.02525-06

Replication and Propagation of Attenuated Vesicular Stomatitis Virus Vectors In Vivo: Vector Spread Correlates with Induction of Immune Responses and Persistence of Genomic RNA▽

Ian D. Simon,[1,2] Jean Publicover,[1,2] and John K. Rose[2]*

Section of Microbial Pathogenesis[1] and Department of Pathology,[2] Yale University School of Medicine, New Haven, Connecticut 06510

Received 15 November 2006/Accepted 16 November 2006

Live-attenuated vesicular stomatitis virus (VSV) vectors expressing foreign antigens induce potent immune responses and protect against viral diseases in animal models. Highly attenuated (VSV-CT1) or single-cycle VSV (VSVΔG) vectors induce immune responses lower than those generated by attenuated wild-type VSV vectors when given intranasally. We show here that reduced spread of the more highly attenuated or single-cycle vectors to other organs, including lymph nodes, correlates with the reduction in the immune responses. A reverse transcription, real-time PCR assay for VSV genomic RNA (gRNA) sequences showed long-term persistence of gRNA from replicating vectors in lymph nodes, long after viral clearance. Such persistence may be important for induction of potent immune responses by VSV vectors.

Vesicular stomatitis virus (VSV), a nonsegmented negative-strand RNA virus, infects cattle, horses, and pigs, causing vesicular lesions. Other mammals, including humans and mice, are also infected in areas of enzootic outbreaks (16, 22). Live-attenuated VSV-based vectors expressing specific foreign proteins produce strong immune responses and protect against viral diseases in many animal models (4–6, 12, 14, 15, 18, 19), including a monkey model for AIDS (3, 11, 17). A live-attenuated VSV vector expressing human immunodeficiency virus proteins is moving into clinical trials as an AIDS vaccine. Given the importance of the VSV vector system, we wanted to determine the extent of vector replication and persistence in vivo.

A recombinant wild-type VSV (rwt) derived from DNA (7) is already attenuated for pathogenesis in mice compared to the wild-type VSV (14). We have also characterized a highly attenuated VSV mutant with a truncation of the VSV G cytoplasmic tail to 1 amino acid (20). This CT1 mutation eliminates all vector-associated pathogenesis after intranasal (i.n.) inoculation of mice (9, 13). Previous studies showed that the VSV-CT1 vector induces humoral and cellular immune responses, but these responses are four- to fivefold lower than those generated by rwtVSV when given i.n. (9). In contrast, the highly attenuated CT1 vector, or a single-cycle vector lacking the VSV G gene (VSVΔG), induced immune responses comparable to rwtVSV when given intramuscularly (10).

Spread of VSV vectors in vivo. We hypothesized that after i.n. immunization, the rwt vector might need to replicate extensively and spread to other organs to induce strong immune responses. To examine the extent of replication of rwtVSV and VSV-CT1 in detail during an in vivo infection, groups of four to seven, 8-week-old BALB/c mice were infected i.n. with 5×10^5 PFU of each virus. We harvested lungs, liver, spleen, plasma, and lymph nodes from mice at various times after infection. We determined virus titers from snap-frozen, homogenized tissue and expressed them as PFU per gram or as PFU/ml in the case of plasma titers (Fig. 1). The brain was omitted from these experiments because a previous study from our lab, focusing on neurotropism of our attenuated, rwtVSV virus, showed that it spread only to the olfactory bulb and no farther into the brain after i.n. administration in young mice (24).

Within the lungs and lymph nodes, we observed the highest titers for rwtVSV at the first time point, 12 h postinfection (hpi) (Fig. 1A and B). In contrast, the peak VSV-CT1 titers in all organs occurred at 24 hpi. At 12 hpi, we recovered a total of 9.5×10^5 PFU rwtVSV from the organs tested. This amount was twice the input virus amount (5×10^5 PFU), a clear indication that the virus was replicating. In contrast, the total amount of VSV-CT1 recovered was less than the input amount. However, the increase in titers from 12 to 24 hpi suggested that VSV-CT1 was replicating after i.n. inoculation but that replication of VSV-CT1 was less efficient than that of rwtVSV in vivo. Our data indicate that VSV-CT1 and rwtVSV replicate and spread in a similar pattern by initially replicating within the lungs and then likely traveling to peripheral organs via the blood. In addition, VSV-CT1 was cleared faster than rwtVSV from the lungs and lymph nodes (Fig. 1A and B). VSV-CT1 reached peak titers nearly as high as rwtVSV in lungs and lymph nodes (Fig. 1), while it grew to titers 10- to 30-fold lower than rwtVSV in tissue culture (20).

We also performed a control experiment to ensure that the CT1 mutant was not reverting in vivo, because the spread in vivo seemed greater than expected based on the 30-fold reduced growth in tissue culture. The deletion of 28 amino acids from the cytoplasmic tail of G in the CT1 mutant is easily detected from the more rapid mobility of the mutant G protein on sodium dodecyl sulfate-polyacrylamide gel electrophoresis

* Corresponding author. Mailing address: Department of Pathology, Yale University School of Medicine, 310 Cedar Street (LH315), New Haven, CT 06510. Phone: (203) 785-6794. Fax: (203) 785-6127. E-mail: john.rose@yale.edu.

▽ Published ahead of print on 6 December 2006.

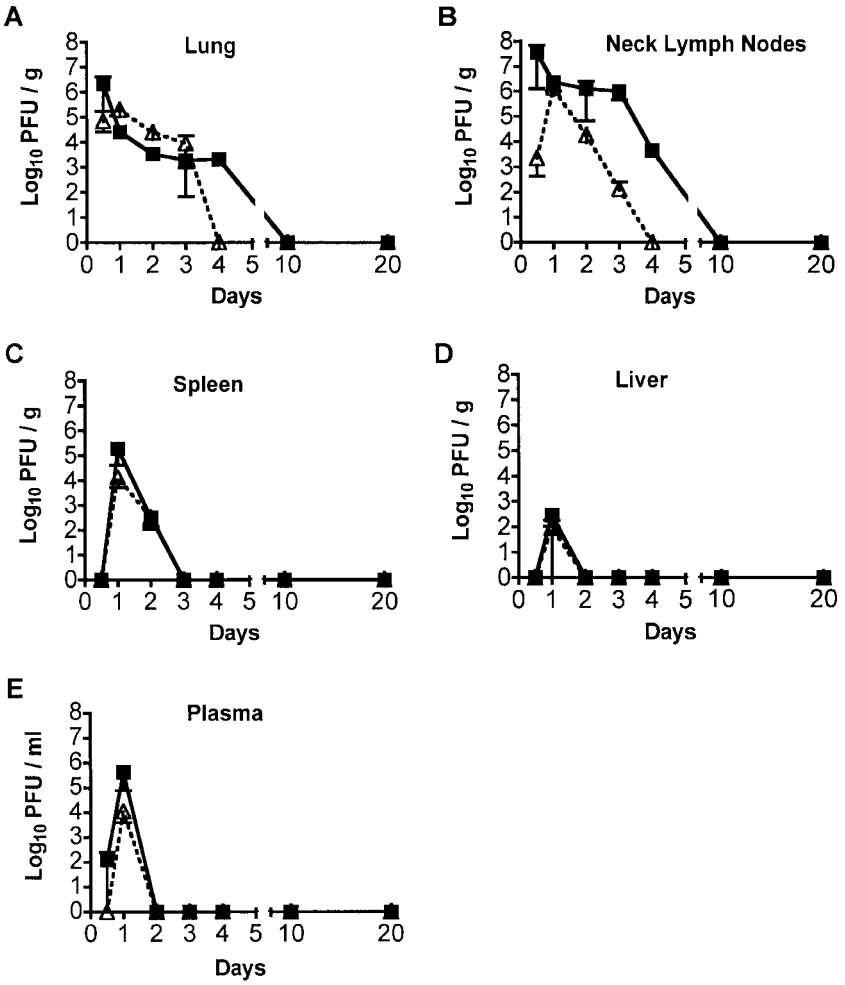

FIG. 1. Replication and spread of recombinant VSV vectors following intranasal inoculation. Eight-week-old BALB/c mice were inoculated with 5×10^5 PFU of rwtVSV (solid squares) and VSV-CT1 (open triangles). Lungs (A), lymph nodes (B), spleen (C), liver (D), and plasma (E) were harvested at various times postinoculation. Virus plaque assays were used to determine viral titers in the indicated tissues. The graph represents average PFU per gram of tissue or per milliliter of plasma ± the standard error of the mean.

(SDS-PAGE). To examine this issue, we infected BHK cells with rwtVSV or VSV-CT1 obtained from lymph nodes harvested at 24 hpi. The stock of virus from these cells was then used to infect BHK-21 cells. At 4 hpi cells were labeled with [^{35}S]methionine for 25 min, and cell lysates were analyzed by SDS-PAGE. As shown in Fig. 2, the CT1 G protein from the recovered virus had a mobility identical to the CT1 G encoded by the input virus and a mobility faster than the rwtVSV G protein. This result indicates that there was no reversion of the mutation after replication in the mouse (20).

Reverse transcription real-time PCR assay. We next developed a reverse transcription, real-time PCR assay for more sensitive detection of VSV genomic RNA (gRNA) in animals and for following spread of the single-cycle ΔG VSV vector that cannot be detected by plaque assay. To generate a standard curve for determination of genome copy number, we isolated gRNA from purified rwtVSV, calculated RNA copy numbers from the RNA concentration and molecular weight of the RNA, and set up reverse transcription reactions using gRNA copy numbers ranging from 10^2 to 10^8 copies. These standard curves showed that we could reliably detect 100 copies of gRNA (Fig. 3F). In the first step of the assay, VSV gRNA was isolated from tissues with a QIAmp vRNA mini kit (Valencia, CA). Then, 1 μg of RNA isolated from each sample and each of the separate standard curve reaction mixtures was reverse transcribed using the N1 forward (plus-strand) primer in a 50-μl reaction mixture. In the second step of the reverse transcription real-time PCR assay, the N1 forward and N2 reverse primers and dual-labeled N3 probe were added to the TaqMan Universal PCR master mix (see the legend to Fig. 3 for primer sequences). Standard curves were included with every experiment. Real-time PCR was carried out on an ABI 7500 real-time sequence detection system (Applied Biosystems).

In addition to the standard curves, we also included the appropriate controls, including reverse-transcribed RNA samples from mock-infected animals and RNA samples from infected animals in which reverse transcriptase was omitted from the reaction mixture. All of these control samples still generated a fluorescent signal detected by the real-time PCR system

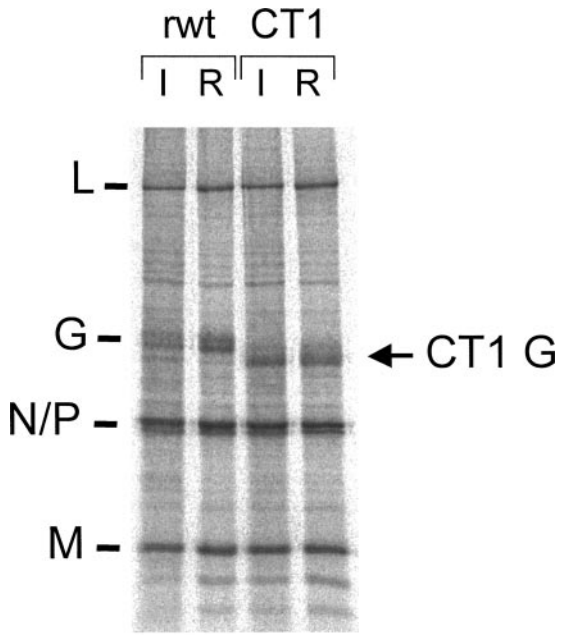

FIG. 2. Proteins expressed by input and recovered viruses. An SDS-PAGE of lysates from BHK cells infected with viruses and labeled with [^{35}S]methionine between 4 and 5 h postinfection is shown. Input (I) viruses are designated VSV(I) and VSV-CT1(I). Viruses indicated VSV(R) and VSV-CT1(R) are viruses recovered from infected lungs at 24 h postinfection. The gel image was collected on a FujiFilm BAS-1800 II system. VSV protein positions are indicated.

but at high (C_T) values that were typically greater than 35. The level we define as background in the assays for gRNA from mice (Fig. 3) represents a threshold cycle number two cycles earlier than detected in any control RNA samples from the same tissue of an uninfected mouse. Four to seven animals were used for each experimental group.

The real-time assay revealed long-term persistence of genomic RNA from replication-competent viruses. Figure 3A to E shows the results of the assays for VSV-CT1 and rwtVSV gRNA in the indicated organs at various times after infection. The highest concentrations of rwtVSV gRNA were found in the lungs and lymph nodes within 24 hpi, while concentrations in the spleen, liver, and plasma were lower and reached their peak by 24 hpi. Interestingly, concentrations of live virus and genome copies per gram of organ were highest within the draining lymph nodes for rwtVSV and VSV-CT1 vectors (Fig. 1B and 3B). There may be an active mechanism for virus concentration in the lymph nodes. Alternatively, virus passively transferred to the lymph node from the bloodstream or lymphatics may actively replicate in the lymph nodes to higher titers than at other sites.

There was a downward trend in gRNA levels after 24 h, just as was seen with the viral titers (Fig. 3A and B), but there were striking differences in the rates of change of virus titers and gRNA levels. For example, within the first 4 days of infection, rwtVSV titers in the lung dropped nearly 1,000-fold (Fig. 1A), while gRNA levels fell only10-fold during the same time period (Fig. 3A). Peak VSV-CT1 titers in the lung dropped from 1.9×10^5 PFU/g at 24 h to undetectable ($<$50 PFU/g) levels by 4 days postinfection (dpi) (Fig. 1A). In contrast, VSV-CT1 gRNA levels dropped less than 10-fold during that same time period (Fig. 3A). The slow kinetics of gRNA decline suggest that it likely persists for even longer times. We considered the possibility that this signal might represent some conversion of viral sequences into DNA by an unknown mechanism. However, this possibility was ruled out by control experiments that left out the reverse transcription step prior to the real-time assay.

A similar pattern of gRNA persisting longer than infectious virus was found in the lymph nodes. Titers of rwtVSV in lymph nodes fell approximately 10,000-fold from 12 h to 4 dpi (Fig. 1B), while the genomic RNA levels peaked at 24 hpi and only declined 5-fold at 4 dpi (Fig. 3B). Genomic RNA levels of VSV-CT1 in the lymph nodes decreased nearly 100-fold from 1 to 4 dpi (Fig. 3B), but infectious VSV-CT1 dropped below detection by 4 dpi (Fig. 1B). Furthermore, we consistently detected low levels of rwtVSV gRNA even at 20 dpi in lung, lymph nodes, spleen, and liver (Fig. 3). In the case of the rwtVSV vector in the lymph nodes and spleen and the VSV-CT1 vector in the lymph nodes, this persistence of gRNA extended for at least 60 dpi (Fig. 3B and C). The levels were typically 1,000- to 10,000-fold lower than levels seen at the peak of infection but were clearly detectable. Results showing persistence of VSV gRNA in mice have not been reported previously. However, persistence of VSV RNA (New Jersey serotype) was detected by nonquantitative PCR in hamsters (1). In cattle infected intradermally on the tongue with VSV New Jersey, RNA was detected in the tongue and draining lymph nodes of infected tissues up to 5 months postinfection (8), long after infectious virus was cleared. The robust immune responses seen after VSV infection of mice may be explained, in part, by the long-term persistence of VSV gRNA and presumably viral proteins in lymph nodes and elsewhere.

The real-time assay showed limited spread and lack of persistence of genomic RNA from single-cycle vectors. To determine if the spreading and persistence of VSV genomes after infection required more than one cycle of virus replication, we used a VSV recombinant (VSVΔG) that lacks the VSV glycoprotein (G) gene. This virus was grown by complementation in cells expressing the VSV G protein (21). The VSVΔG virus infects cells and undergoes only a single round of replication because it does not produce virus particles capable of infecting other cells.

We inoculated mice i.n. with 5×10^5 PFU of VSVΔG, harvested organs at various times postinfection, and assayed them for the presence of gRNA just as in the previous experiments. Within the lung, levels of VSVΔG gRNA were similar to VSV-CT1 levels throughout the time course (Fig. 3A). However, in contrast to VSV-CT1 and rwtVSV, the single-cycle virus did not spread to other organs except for lymph nodes. There it was present only transiently during the first 4 days, at levels close to background (Fig. 3B). We conclude that significant spreading to other organs after intranasal inoculation requires more than one cycle of virus replication. The fact that only a low level of RNA from the single-cycle VSVΔG vector appeared in these lymph nodes indicates that active replication plays an important role in virus concentration in lymph nodes.

Vector immune responses correlate with extent of virus spread and persistence. The cellular immune responses generated by the rwt, CT1, and ΔG vectors correlate with the

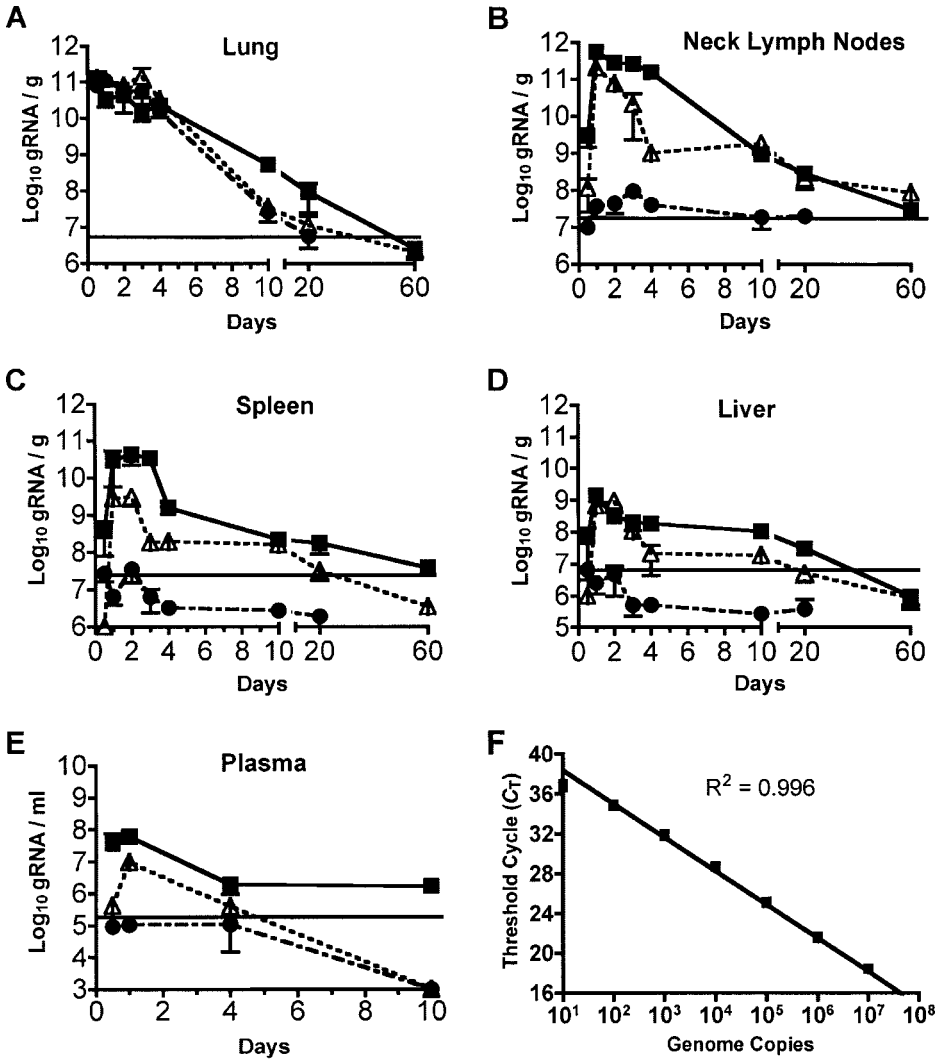

FIG. 3. Spread and persistence of genomic RNA following intranasal inoculation. Eight-week-old BALB/c mice were inoculated with 5×10^5 PFU of rwtVSV (solid squares), VSV-CT1 (open triangles), and VSVΔG (solid circles). At various times postinoculation, lungs (A), lymph nodes (B), spleen (C), liver (D), and plasma (E) were harvested. Real-time PCR was carried out using N1 forward (5′-GATAGTACCGGAGGATTG ACGACTA-3′) and N2 reverse (3′-TCAAACCATCCGAGCCATTC-5′) primers and dual-labeled N3 probe (5′–carboxyfluorescein-TGCACC GCCACAAGGCAGAGA–6-carboxytetramethylrhodamine–3′). The graph represents the average number of genome copies per gram of tissue or per milliliter of plasma ± the standard error of the mean. Horizontal lines indicate the levels we defined as the background, representing a threshold cycle number of two cycles earlier than detected in any control RNA samples from the same tissue of an uninfected mouse.

extent of replication and spread seen here. The primary cellular immune responses (measured using major histocompatibility complex [MHC] I tetramers) generated by the rwt vector are about four- to fivefold higher than those generated by the CT1 vector after intranasal inoculation (9). Responses to the single-cycle ΔG vector given i.n. are even lower still (10). The reduced ability of the highly attenuated and single-cycle vectors to spread to sites such as lymph nodes and spleen and prime immune responses after i.n. inoculation is likely the reason for the reduced responses. However, all three vectors generate strong and comparable cellular immune responses when given intramuscularly (10), suggesting that spread from the muscle to sites where immune responses are generated might be a much more efficient process than spread from the lung.

Possible models for persistence of VSV genomic RNA. Persistence of VSV genomic RNA long after infectious virus is cleared could be explained by two models. In the first model, there would be a low level of long-term replication that persists in just a few cells, perhaps in the lymph nodes. However, VSV infection generates rapid and potent cellular immune responses, and cells harboring replicating VSV would have to be resistant to attack by T cells. VSV infection also induces neutralizing antibody production by 7 dpi (I. D. Simon and J. K. Rose, unpublished results). Any infectious virus produced should therefore be neutralized and the infectious cycle stopped. We therefore favor a second model in which whole virus particles or nucleocapsids containing RNA are trapped, for example, in the lymph node capsule, and cleared very slowly. There is also a hybrid

model in which virus is trapped and occasionally released to cause an infection.

We have attempted to distinguish among these models by developing a real-time assay highly specific for positive-strand VSV mRNA sequences present only in infected cells and not in virions. If mRNA sequences were persisting long term, it would be an indication that replication was also persisting. So far we have not been able to develop a VSV mRNA-specific assay that does not also detect positive-strand RNA sequences in RNA purified from virions. This RNA may represent full-length antigenomic RNA packaged in virions. Packaging of antigenomic RNA has been reported for rabies virus, a distant relative of VSV in the rhabdovirus family (2).

Neutralizing antibody titers to VSV continue to increase for up to 90 days after intranasal infection of mice and persist for 2 years (a mouse life span), often with only two- to fourfold decreases in titer (J. K. Rose, unpublished results). The increase in neutralizing antibody titer presumably involves selection for B cells producing higher-affinity antibodies to VSV G protein. This selection could be driven by persistence of G protein in lymph nodes. Recent studies from Turner et al. (23) using a sensitive assay for activation of antigen-specific T cells have shown persistence of VSV-encoded antigen in mouse lymph nodes for at least 6 weeks following an acute VSV infection. These findings are consistent with our findings of persistence of VSV gRNA sequences in lymph nodes. Such persistence of low levels of viral genomes and virus-encoded antigens could help explain potent immune responses and often lifelong immunity generated following acute viral infections.

This work was supported by NIH grant R37-AI40357 to J.K.R.

REFERENCES

1. **Barrera, J. C., and G. J. Letchworth.** 1996. Persistence of vesicular stomatitis virus New Jersey RNA in convalescent hamsters. Virology **219:**453–464.
2. **Conzelmann, K. K., and M. Schnell.** 1994. Rescue of synthetic genomic RNA analogs of rabies virus by plasmid-encoded proteins. J. Virol. **68:**713–719.
3. **Egan, M. A., S. Y. Chong, N. F. Rose, S. Megati, K. J. Lopez, E. B. Schadeck, J. E. Johnson, A. Masood, P. Piacente, R. E. Druilhet, P. W. Barras, D. L. Hasselschwert, P. Reilly, E. M. Mishkin, D. C. Montefiori, M. G. Lewis, D. K. Clarke, R. M. Hendry, P. A. Marx, J. H. Eldridge, S. A. Udem, Z. R. Israel, and J. K. Rose.** 2004. Immunogenicity of attenuated vesicular stomatitis virus vectors expressing HIV type 1 Env and SIV Gag proteins: comparison of intranasal and intramuscular vaccination routes. AIDS Res. Hum. Retrovir. **20:**989–1004.
4. **Jones, S. M., H. Feldmann, U. Stroher, J. B. Geisbert, L. Fernando, A. Grolla, H. D. Klenk, N. J. Sullivan, V. E. Volchkov, E. A. Fritz, K. M. Daddario, L. E. Hensley, P. B. Jahrling, and T. W. Geisbert.** 2005. Live attenuated recombinant vaccine protects nonhuman primates against Ebola and Marburg viruses. Nat. Med. **11:**786–790.
5. **Kahn, J. S., A. Roberts, C. Weibel, L. Buonocore, and J. K. Rose.** 2001. Replication-competent or attenuated, nonpropagating vesicular stomatitis viruses expressing respiratory syncytial virus (RSV) antigens protect mice against RSV challenge. J. Virol. **75:**11079–11087.
6. **Kapadia, S. U., J. K. Rose, E. Lamirande, L. Vogel, K. Subbarao, and A. Roberts.** 2005. Long-term protection from SARS coronavirus infection conferred by a single immunization with an attenuated VSV-based vaccine. Virology **340:**174–182.
7. **Lawson, N. D., E. A. Stillman, M. A. Whitt, and J. K. Rose.** 1995. Recombinant vesicular stomatitis viruses from DNA. Proc. Natl. Acad. Sci. USA. **92:**4477–4481.
8. **Letchworth, G. J., J. C. Barrera, J. R. Fishel, and L. Rodriguez.** 1996. Vesicular stomatitis New Jersey virus RNA persists in cattle following convalescence. Virology **219:**480–484.
9. **Publicover, J., E. Ramsburg, and J. K. Rose.** 2004. Characterization of nonpathogenic, live, viral vaccine vectors inducing potent cellular immune responses. J. Virol. **78:**9317–9324.
10. **Publicover, J., E. Ramsburg, and J. K. Rose.** 2005. A single-cycle vaccine vector based on vesicular stomatitis virus can induce immune responses comparable to those generated by a replication-competent vector. J. Virol. **79:**13231–13238.
11. **Ramsburg, E., N. F. Rose, P. A. Marx, M. Mefford, D. F. Nixon, W. J. Moretto, D. Montefiori, P. Earl, B. Moss, and J. K. Rose.** 2004. Highly effective control of an AIDS virus challenge in macaques by using vesicular stomatitis virus and modified vaccinia virus Ankara vaccine vectors in a single-boost protocol. J. Virol. **78:**3930–3940.
12. **Reuter, J. D., B. E. Vivas-Gonzalez, D. Gomez, J. H. Wilson, J. L. Brandsma, H. L. Greenstone, J. K. Rose, and A. Roberts.** 2002. Intranasal vaccination with a recombinant vesicular stomatitis virus expressing cottontail rabbit papillomavirus L1 protein provides complete protection against papillomavirus-induced disease. J. Virol. **76:**8900–8909.
13. **Roberts, A., L. Buonocore, R. Price, J. Forman, and J. K. Rose.** 1999. Attenuated vesicular stomatitis viruses as vaccine vectors. J. Virol. **73:**3723–3732.
14. **Roberts, A., E. Kretzschmar, A. S. Perkins, J. Forman, R. Price, L. Buonocore, Y. Kawaoka, and J. K. Rose.** 1998. Vaccination with a recombinant vesicular stomatitis virus expressing an influenza virus hemagglutinin provides complete protection from influenza virus challenge. J. Virol. **72:**4704–4711.
15. **Roberts, A., J. D. Reuter, J. H. Wilson, S. Baldwin, and J. K. Rose.** 2004. Complete protection from papillomavirus challenge after a single vaccination with a vesicular stomatitis virus vector expressing high levels of L1 protein. J. Virol. **78:**3196–3199.
16. **Rose, J. K., and M. A. Whitt.** 2001. Rhabdoviridae: the viruses and their replication, 4th ed., vol. 1. Lippincott-Raven, New York, N.Y.
17. **Rose, N. F., P. A. Marx, A. Luckay, D. F. Nixon, W. J. Moretto, S. M. Donahoe, D. Montefiori, A. Roberts, L. Buonocore, and J. K. Rose.** 2001. An effective AIDS vaccine based on live attenuated vesicular stomatitis virus recombinants. Cell **106:**539–549.
18. **Schlereth, B., L. Buonocore, A. Tietz, V. ter Meulen, J. K. Rose, and S. Niewiesk.** 2003. Successful mucosal immunization of cotton rats in the presence of measles virus-specific antibodies depends on degree of attenuation of vaccine vector and virus dose. J. Gen. Virol. **84:**2145–2151.
19. **Schlereth, B., J. K. Rose, L. Buonocore, V. ter Meulen, and S. Niewiesk.** 2000. Successful vaccine-induced seroconversion by single-dose immunization in the presence of measles virus-specific maternal antibodies. J. Virol. **74:**4652–4657.
20. **Schnell, M. J., L. Buonocore, E. Boritz, H. P. Ghosh, R. Chernish, and J. K. Rose.** 1998. Requirement for a non-specific glycoprotein cytoplasmic domain sequence to drive efficient budding of vesicular stomatitis virus. EMBO J. **17:**1289–1296.
21. **Schnell, M. J., J. E. Johnson, L. Buonocore, and J. K. Rose.** 1997. Construction of a novel virus that targets HIV-1-infected cells and controls HIV-1 infection. Cell **90:**849–857.
22. **Tesh, R. B., P. H. Peralta, and K. M. Johnson.** 1969. Ecologic studies of vesicular stomatitis virus. I. Prevalence of infection among animals and humans living in an area of endemic VSV activity. Am. J. Epidemiol. **90:**255–261.
23. **Turner, D. L., L. S. Cauley, K. M. Khanna, and L. Lefrançois.** 2007. Persistent antigen presentation after acute vesicular stomatitis virus infection. J. Virol. **81:**2039–2046.
24. **van den Pol, A. N., K. P. Dalton, and J. K. Rose.** 2002. Relative neurotropism of a recombinant rhabdovirus expressing a green fluorescent envelope glycoprotein. J. Virol. **76:**1309–1327.